Adaptive Multi-sensing in EH-WSN for Smart Environment

Vini Gupta and Swades De
Department of Electrical Engineering and Bharti School of Telecommunication, IIT Delhi, New Delhi, India

***Abstract*—This paper proposes a novel multi-sensing framework for an energy harvesting heterogeneous wireless sensor network. This framework has utility in smart environment application of Internet-of-Things. It considers a network of multiple wireless nodes, each having heterogeneous sensors to sense slowly-varying environment parameters. For monitoring each parameter, the developed strategy adaptively selects the corresponding sensors of a few neighboring nodes for activation, which jointly optimizes the sensing accuracy and energy efficiency. This process effectively activates a subset of sensors at each node. The subset of selected field nodes as well as the activated sensors at each node in the field is dynamically updated, as a function of harvested energy availability and sensing quality. Simulation results demonstrate the energy efficiency and sensing quality of the proposed framework.**

***Index Terms*—Adaptive multi-sensing, energy harvesting-wireless sensor networks (EH-WSNs), network residual energy**

I. Introduction

Smart environment [1] demands heterogeneous wireless sensor networks (WSNs) that can simultaneously sense multiple spatio-temporally varying environment parameters. However, this multi-sensing activity is expected to be energy-intensive, which is a critical resource for battery-constrained wireless nodes. Therefore, an intelligent multi-sensing framework is required that enables sparsely sensing environment parameters such that their inference accuracy and network's energy efficiency are jointly optimized. Although node-level optimization increases lifespan of the nodes, due to limited battery capacity these nodes are bound to become energy-depleted at some point of operation. Replacing batteries of such nodes, or on-demand energy replenishment, as suggested in [2], [3], are not always practical. Instead, using nodes that can harvest ambient solar energy [4], [5] will impart energy-sustainability in energy-hungry multi-sensing applications.

A. Related Works

Several approaches have been proposed for sensing single parameter of a process monitored by a WSN. Most of them exploit spatio-temporal nature of signal pertaining to the observed process and sense it using a few nodes only. Conventional approaches in [6], [7] randomly select such nodes. Thereafter, sensor selection techniques which activate a fixed number of nodes to ensure certain energy efficiency [8] or sensing accuracy [9]–[11] or both [12], [13], have gained significant research interest. However, these fixed active nodes based-schemes are impractical for monitoring a spatio-temporally varying process. This limitation has motivated the development of adaptive sensing schemes in [14], [15]. In such approaches, the number of nodes to be activated is adapted according to dynamics of the evolving process. In this context, an adaptive and energy-efficient single parameter sensing framework was developed in [16] that collectively considers process dynamics, sensing quality, and each node's energy resource for optimized sensor selection.

Large-scale WSNs incur high deployment and maintenance cost. Monolithic sensing approaches, as in [6]–[16], do not fully harness the capabilities of sensor-rich environment. Further, the concept of smart environment demands accurate monitoring of multiple parameters. Deploying dedicated nodes for sensing these different parameters results in inefficient resource utilization. To this end, deployment of WSNs that can be shared for sensing multiple environment parameters (i.e. multi-sensing) has been considered in a few existing works. In a shared network setting, it is possible to process multiple sensed parameters in parallel, resulting in timeliness of operations. In this context, a multi-sensor proposal was suggested in [17] that increases the capabilities of intelligent systems by sensing various environmental parameters. The work in [18] developed a multi-sensing platform that uses temperature and gas sensors. The authors in [19] developed a low-cost design of a sensor node for multichannel data acquisition. In [5], threshold-based protocols were designed for energy-efficiency in a heterogeneous sensor system. Similarly, in [20], the authors proposed wavelet-based adaptive and hierarchical sampling models for sensing different dependent parameters.

B. Research Gap and Motivation

Notably, the multi-sensing designs and proposals [17]–[19] do not focus on sensor selection criterion and parameter estimation strategy. The works in [5], [20] focused on strategies for selecting multiple heterogeneous sensors. However, these works considered a limiting scenario of sensing dependent parameters which enables development of hierarchical sensing strategies. Threshold-based sensor selection strategies developed therein have the associated uncertainty, as they are based on measured signal values corrupted by unobserved noise. Moreover, these works do not provide estimate of the monitored parameters, and they do not consider remaining energy of different nodes during the selection process, which may leads to energy-inefficient sensor selection. Thus, so far none of the existing works on multi-sensing select sensors by jointly optimizing sensing quality and network energy efficiency. In context of energy efficiency it may also be noted

that, the remaining energy of sensor nodes could be time-varying, as in ambient energy harvesting-capable nodes.

To fill these research gaps, this work formulates a novel adaptive and energy-efficient multi-sensing paradigm for energy harvesting heterogeneous WSN-based smart environment applications. It considers dynamics of the monitored parameters and jointly optimizes the sensing accuracy and network energy efficiency to activate a subset of sensors of the nodes in the network. Unlike hierarchical sensing, it has considered a challenging scenario where monitored parameters do not depend on each other. The developed strategy provides an error-bounded estimate of the parameters across the network by using measurements of a few sensors of the deployed nodes.

C. Contributions

Key contributions of this work are as follows: 1) The proposed multi-sensing framework is adaptive to the node-level stochastic energy availability. 2) It selects a subset of heterogeneous sensors mounted on wireless nodes for sensing slowly-varying environmental parameters in an energy-efficient manner without compromising on sensing quality. For this, a critical trade-off between the sensing quality and network energy efficiency is jointly optimized. 3) A generic procedure for synthetically generating environmental parameters of interest with different spatial and temporal correlations is outlined. 4) Simulation results illustrate that the proposed framework offers energy saving without sacrificing the sensing quality, and it performs consistently better compared to the closest existing sensor selection framework that can be used for multi-sensing. Applications of the proposed framework: smart environment, smart agriculture, pollution monitoring.

D. Organization

The paper layout is as follows. Components of the energy harvesting-WSN (EH-WSN) system model, namely, signal generation, acquisition, and solar harvesting model, are presented in Section II. Section III describes the proposed adaptive multi-sensing framework, followed by simulation results and concluding remarks, respectively in Sections IV and V.

II. EH-WSN System Model

A. Signal Acquisition

Consider an EH-WSN deployed with N wireless nodes each containing P different sensors for monitoring P slowly-varying environmental parameters of interest (such as SO_2, NO_2, CO pollutants) as depicted in Fig. 1. These sensors have different detection limits. To-be-monitored P parameters do not depend on each other. Each node is considered equipped with solar energy harvester module. Let $\mathbf{z}_k^p = [z_k^p(1), \cdots, z_k^p(N)]^T \in \mathbb{R}^{N\times 1}$ represent a spatial signal vector corresponding to values of p^{th} parameter $(1 \le p \le P)$ across N nodes during k^{th} measurement cycle. Utilizing spatial correlation inherent in the slowly-varying p^{th} parameter across N nodes, it can be monitored using the p^{th} sensor of a few nodes. Let the fusion center (FC) selects $M_k^p\,(\le N)$ number of nodes with p^{th} sensor

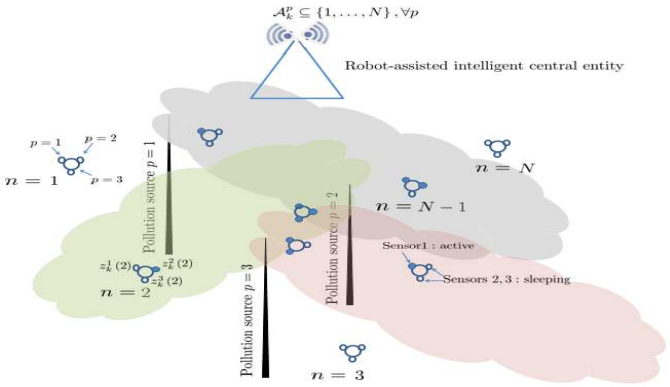

Fig. 1: EH-WSN for multi-sensing.

active during the k^{th} cycle. These nodes constitute active set $\mathcal{A}_k^p \subseteq \{1, \cdots, N\}$. Thus, $|\mathcal{A}_k^p| = M_k^p$. The active sensor set selection for different parameters is done at the FC by running multiple optimization problems in parallel (discussed in Section. III). The resulting activation schedule is conveyed to the respective nodes. Sensing status (on/off) of the p^{th} sensors of all nodes be captured in a binary sensing matrix $\mathbf{A}_k^p \in \mathbb{R}^{M_k^p \times N}$. Each row corresponds to one active sensor, i.e., $\mathbf{A}_k^p(m,n) = \begin{cases} 1 & , n = i \;\text{ s.t. } i \in \mathcal{A}_k^p \\ 0 & , n \in \{1,\ldots,N\}\backslash\{i\} \end{cases}, \forall 1 \le m \le M_k^p$. The p^{th} parameter signal, measured by the corresponding sensors of nodes $\in \mathcal{A}_k^p$, is represented by measurement vector $\widetilde{\mathbf{y}}_k^p \in \mathbb{R}^{M_k^p \times 1}$. Thus, signal model for acquiring the p^{th} environmental parameter, $\forall 1 \le p \le P$, is given by,

$$\widetilde{\mathbf{y}}_k^p = \mathbf{A}_k^p \mathbf{z}_k^p + \mathbf{n}_k^p, \tag{1}$$

where $\mathbf{n}_k^p \in \mathbb{R}^{M_k^p \times 1}$ is white Gaussian noise vector with independent and identically distributed components of zero mean and variance σ^2. The measured signals corresponding to all the parameters are collected from the nodes by a mobile robot which delivers them to the FC so as to save nodes' energy required for transmission. The FC, then, estimates the parameter signals across all the nodes $(\mathbf{z}_k^p, \forall\ p)$ and carries sensor selection process for next cycle. Similar to the work [16], sparse representation of the signal model (1) is given by (2) using principal component analysis (PCA) [21],

$$\mathbf{y}_k^p = \mathbf{A}_k^p \mathbf{B}_k^p \mathbf{x}_k^p + \mathbf{n}_k^p, \tag{2}$$

where $\mathbf{B}_k^p \in \mathbb{R}^{N\times N}$ is sparsification matrix, $\mathbf{x}_k^p \in \mathbb{R}^{N\times 1}$ is sparse vector, and $\mathbf{y}_k^p \in \mathbb{R}^{M_k^p \times 1}$ is equivalent measurement vector. In PCA, a few past instances of the signals $\mathbf{z}_k^p, \forall p$, are used as training sets $(\mathcal{T}^p, \forall p)$ before start of the sensing operation. These sets are updated in each cycle using current cycle's estimates of the signal $\mathbf{z}_k^p, \forall p$.

B. Signal Generation

Let the strength of random signal generated from s^{th} source of parameter p during k^{th} measurement cycle be $u_k^p(s)$, $1 \le p \le P$, $1 \le s \le S^p$, where S^p is the total number of sources of parameter p. Its temporal samples are generated using AR(1) process [16] as $u_{k+1}^p(s) =$

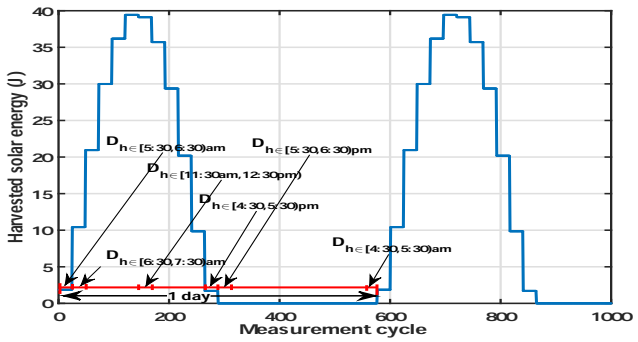

Fig. 2: Solar energy harvested by nodes in each cycle.

$\varphi^p u_k^p(s) + \sqrt{1-(\varphi^p)^2} w_{k+1}^p(s)$, where φ^p represents temporal correlation between two consecutive samples of $u_{(\cdot)}^p(s)$, $w_{k+1}^p(s) \sim \mathcal{N}\left(0, \sigma^2_{u_k^p}(s)\right)$, and $\sigma^2_{u_k^p}(s)$ represents the variance of $u_k^p(s)$. The corresponding signal across different nodes is: $z_k^p(n) = \sum_{s=1}^{S^p} e^{-\frac{d_{n,s}}{\theta^p}} u_k^p(s)$ [16], where $d_{n,s}$ and θ^p respectively denote distance between n^{th} node and s^{th} source and spatial diffusion parameter. This method is used to generate spatio-temporal samples of the environmental parameters with different temporal and spatial correlation characteristics.

C. Solar Energy Harvesting Model

Energy harvested by a solar panel is given by [22],

$$E_{h_k} = D_k \times \eta \times S_{pv} / \Delta T, \tag{3}$$

where D_k, η, S_{pv}, and ΔT respectively denote solar irradiance (KWh/m^2), photovoltaic (PV) cell efficiency in solar panel, panel size (m^2), and slot duration (min). In this work, slot duration is set as 2.5min, which corresponds to combined average time of one measurement cycle [16] and sensor response time [23]. η and S_{pv} are respectively set as 12.8% and 0.0168m^2 [22]. Hourly solar irradiance (D_h) in the month of October for Delhi, as an example, is obtained from the study in [24]. Since the granularity of solar irradiance data is one hour, D_k is assumed constant for all the slots within an hour interval, i.e., $D_k = D_h = \begin{cases} 0.036, & h \in [6:30-7:30)\,\text{am (or } 1 \le k \le 24) \\ 0.202, & h \in [7:30-8:30)\,\text{am (or } 25 \le k \le 48) \end{cases}$, likewise, as shown in Fig. 2.

D. Remaining Energy Update

Energy of a node per measurement cycle is updated as:

$$Erem_k(n) = Erem_{k-1}(n) - Es_k(n) + E_{h_k}, \tag{4}$$

$$Es_k(n) = \sum_{p=1}^{P} E_s^p \times \mathbf{1}\left(n \in \mathcal{A}_k^p\right), \tag{5}$$

where $Es_k(n)$ represents the total sensing energy consumed by the active sensors of n^{th} node, E_s^p denotes the sensing energy consumed by p^{th} sensor, and the indicator function $\mathbf{1}\left(n \in \mathcal{A}_k^p\right) = \begin{cases} 1, & \text{if } n \in \mathcal{A}_k^p \\ 0, & \text{if } n \notin \mathcal{A}_k^p \end{cases}$. It is assumed that the energy information is sent to the FC along with measured signals.

III. Adaptive Multi-sensing Framework

For each environment parameter, the FC runs adaptive sensor selection and signal estimation tasks in parallel during each measurement cycle. For the latter task, it obtains an estimate of the p^{th} sparse signal, represented as $\widehat{\mathbf{x}}_k^p$, using the vector $\mathbf{y}_k^p$ and matrices $\mathbf{A}_k^p, \mathbf{B}_k^p$ of (2) by employing sparse Bayesian learning (SBL) framework [25]. Estimate of the parameter signal $\widehat{\mathbf{z}}_k^p$ is obtained from $\widehat{\mathbf{x}}_k^p$ using PCA transformation and $\mathbf{B}_k^p$ [16]. The active nodes across which the p^{th} parameter signal (i.e. $z_k^p(\cdot)$) is below detection limit (ρ^p) of the respective sensors constitute a set $\mathcal{I}_k^p$. Note that, either $\mathcal{I}_k^p \subseteq \mathcal{A}_k^p$ or $\mathcal{I}_k^p = \phi$. Measured signal across p^{th} sensors of such nodes are not used in the recovery task because $y_k^p(n) = 0, \forall n \in \mathcal{I}_k^p$. Such an integration of system's constraint in the recovery and sensing tasks (discussed next) has immense practical significance in heterogeneous sensing scenarios, which is still missing in the existing literature.

To find active sensors of nodes for sensing P parameters in each $(k+1)^{th}$ cycle, P multi-objective optimization problems (MOPs) (6) are solved in parallel using scalarization technique [26]. MOP proposed in [16] for monolithic sensing is modified to include the heterogeneous sensing constraint as follows:

$$\underset{\widetilde{\mathbf{A}}_{k+1}^p(n,n)\ \forall n}{\text{minimize}} \quad \left(1-\lambda_{k+1}^p\right) \text{Tr}\left\{\left(\frac{1}{\sigma^2}\left(\mathbf{B}_{k+1}^p\right)^T \widetilde{\mathbf{A}}_{k+1}^p \left(\mathbf{B}_{k+1}^p\right) + \left(\mathbf{\Gamma}_{k+1}^p\right)^{-1}\right)^{-1}\right\}$$
$$+ \lambda_{k+1}^p \left(\sum_{n=1}^{N} \frac{1}{Erem_k(n)} \widetilde{\mathbf{A}}_{k+1}^p(n,n)\right)$$

$$\text{subject to} \quad \widetilde{\mathbf{A}}_{k+1}^p(n,n) \in [0,1], \ n = 1, \ldots, N \tag{6a}$$
$$\widetilde{\mathbf{A}}_{k+1}^p(n,n) = 0, \ n \in \{i \mid Erem_k(i) = 0\} \tag{6b}$$
$$\sum_{j \in \mathcal{R}_r} \widetilde{\mathbf{A}}_{k+1}^p(j,j) \ge 1, \ r = 1, \ldots, R \tag{6c}$$
$$\widetilde{\mathbf{A}}_{k+1}^p(n,n) = 0, \ n \in \mathcal{I}_{k+1|k}^p. \tag{6d}$$

Bayesian Cramér-Rao bound, $\text{BCRB} = \text{Tr}\left\{\left(\frac{1}{\sigma^2}\left(\mathbf{B}_{k+1}^p\right)^T \left(\mathbf{A}_{k+1}^p\right)^T \mathbf{A}_{k+1}^p \mathbf{B}_{k+1}^p + \left(\mathbf{\Gamma}_{k+1}^p\right)^{-1}\right)^{-1}\right\}$, characterizes unknown mean squared error [16]. The entity $\left(\mathbf{A}_{k+1}^p\right)^T \mathbf{A}_{k+1}^p$ forms a binary diagonal matrix $\widetilde{\mathbf{A}}_{k+1}^p \in \mathbb{R}^{N \times N}$ with $\widetilde{\mathbf{A}}_{k+1}^p(n,n) = 1/0$ denoting active/sleeping p^{th} sensor of the n^{th} node. The function $\sum_{n=1}^{N} \frac{1}{Erem_k(n)} \widetilde{\mathbf{A}}_{k+1}^p(n,n)$ promotes sparse sensor selection with more weight given to sensors of nodes with higher remaining energy after k^{th} cycle, i.e. $Erem_k(\cdot)$. Thus, (6) jointly optimizes sensing quality and network energy efficiency. Relaxed constraint (6a) signifies active(1)/sleep(0) state of p^{th} sensor of n^{th} node. Constraint (6b) represents the fact that sensors of the node(s) with zero remaining energy cannot participate. For better monitoring of parameter and its recovery, constraint (6c) ensures selection of p^{th} sensor of at least one node from each coverage region $\mathcal{R}_r, \forall\ 1 \le r \le R$. Here, it is assumed that the WSN field is divided into R fixed non-overlapping regions. Detection limit constraint (6d) forbids selection of p^{th} sensor of nodes belonging to predicted set $\mathcal{I}_{k+1|k}^p$. This set contains nodes across which the environment parameter signal $z_{k+1}^p(\cdot)$ may remain below

the sensor's detection limit. Its construction is discussed next along with the adaptation mechanism. Scalarized MOP (6) is solved using CVX [27], given λ_{k+1}^p in each measurement cycle; the unknown entities M_{k+1}^p and $\mathcal{A}_{k+1}^p$ are obtained as,

$$M_{k+1}^p = \text{round}\left(\sum_{n=1}^{N} \widetilde{\mathbf{A}}_{k+1}^p(n,n)\right), \quad (7)$$

$$\mathcal{A}_{k+1}^p = \text{Row indices of } M_{k+1}^p \text{ largest elements of set: } \left\{\widetilde{\mathbf{A}}_{k+1}^p(n,n) | \widetilde{\mathbf{A}}_{k+1}^p(n,n) \geq \widetilde{\mathbf{A}}_{k+1}^p(m,m)\, \forall n,m\right\} \quad (8)$$

λ_{k+1}^p is obtained by employing modified binary search (MBS) proposed in [16] with the difference that, now an additional input $\mathcal{I}_{k+1|k}^p$ is passed and the MOP (6) is solved. MBS minimizes (6) by searching λ_{k+1}^p in space $[0,1]$ with stopping criteria $(\lambda_{k+1}^p)_U - (\lambda_{k+1}^p)_L < \Delta$ or $\sum_{n=1}^{N} \widetilde{\mathbf{A}}_{k+1}^p(n,n) == M_{k+1|k}^p$; Δ being a small positive real number. Input $M_{k+1|k}^p$ to the MBS algorithm represents the number of nodes predicted to have p^{th} active sensor in $(k+1)^{th}$ cycle. It is adapted based on estimated variation of p^{th} parameter in the previous cycle k denoted by $(\widehat{\delta}_k^p)$ and updated energy resources of nodes such that the BCRB remains within a given application-specific acceptable range $[\alpha, \beta]$. Intuitively, higher parameter variation demands more active sensors. Thus, if $\widehat{\delta}_k^p > \delta_{th}^p$, then $M_{k+1|k}^p \leftarrow M_k^p + 1$, where $\widehat{\delta}_k^p = \frac{\|\widehat{\mathbf{z}}_k^p - \widehat{\mathbf{z}}_{k-1}^p\|}{\sqrt{N}}$ and δ_{th}^p is an appropriate threshold. Else, decrease M_k^p in unit steps $(M_{k+1|k}^p \leftarrow M_k^p - i, \forall i = 1, \cdots, M_k^p - R)$ to create pruned active set $\mathcal{A}_{k|M_k^p-i}^p$ (i.e. $\mathcal{A}_k^p \setminus \{i \text{ nodes}\}$) and compute a heuristic $\widehat{\epsilon}_k^{p\,1} = \left\|\widehat{\mathbf{x}}_k^p - \widehat{\mathbf{x}}_{k|M_k^p-i}^p\right\|$. If $\widehat{\epsilon}_k^p \leq \epsilon_{th}^p$ and corresponding $\text{BCRB}_{k|M_k^p-i}^p \in [\alpha, \beta]$, further decrease M_k^p until either $\text{BCRB}_{k|M_k^p-i}^p \notin [\alpha, \beta]$ or $M_k^p - i < R$. Considering the set $\mathcal{I}_k^p$ and slowly varying nature of environment parameter, $\mathcal{I}_{k+1|k}^p$ and $M_{k+1|k}^p$ are updated as,

$$\begin{Bmatrix} \mathcal{I}_{k+1|k}^p \leftarrow \phi, \text{ if } \mathcal{I}_k^p = \phi \\ \mathcal{I}_{k+1|k}^p \leftarrow \mathcal{I}_k^p, \text{if } \mathcal{I}_k^p \neq \phi, \widehat{\delta}_k^p \leq \delta_{th}^p \\ \mathcal{I}_{k+1|k}^p \leftarrow \phi, \text{if } \mathcal{I}_k^p \neq \phi, \widehat{\delta}_k^p > \delta_{th}^p \end{Bmatrix}, M_{k+1|k}^p = \min\{M_k^p, N - |\mathcal{I}_k^p|\} \quad (9)$$

Next, after running the MBS, if $\sum_{n=1}^{N} \widetilde{\mathbf{A}}_{k+1}^p(n,n) = M_{k+1|k}^p$, compute BCRB_{k+1} corresponding to the output $(\widetilde{\mathbf{A}}_{k+1}^p)$. If $\text{BCRB}_{k+1} \in [\alpha, \beta]$, proceed with next measurement cycle's sensing process. Otherwise, for cases $\text{BCRB}_{k+1} < \alpha$ (or $> \beta$), update $M_{k+1|k}^p \leftarrow \max\left\{M_{k+1|k}^p - 1, R\right\}$ $\left(\text{or } \min\left\{M_{k+1|k}^p + 1, N\right\}\right)$.

A step by step description of the proposed adaptive multi-sensing framework is outlined in Algorithm 1 which runs parallely at the FC for each environment parameter p.

Algorithm 1 Adaptive multi-sensing framework

Input: $\mathcal{T}^p = \{\mathbf{z}_{-K_{tr}+1}^p, \ldots, \mathbf{z}_{-1}^p, \mathbf{z}_0^p\}, \mathcal{R}_r \forall r, \alpha, \beta, \delta_{th}^p, \epsilon_{th}^p, \rho^p$.
Initialization: $\mathbf{Erem}_1, \lambda_1^p, k=1, exitflag^p = 0, \mathcal{I}_1^p = \phi$.
while $exitflag^p == 0$ **do**
  if $k = 1$ **then**
    -Calculate $\mathbf{B}_k^p$ using PCA scheme [16].
    -Solve (6) to get $M_k^p, \mathcal{A}_k^p$, obtain $\mathbf{A}_k^p$ (Sec. II-A).
  end if
  Broadcast sensing schedule $\mathcal{A}_k^p$, collect $\mathbf{y}_k^p$.
  Find $\mathcal{I}_k^p$. Use $\{y_k^p(n), n \in \mathcal{A}_k^p \backslash \mathcal{I}_k^p\}$, SBL [25] to get $\widehat{\mathbf{x}}_k^p$.
  Obtain $\widehat{\mathbf{z}}_k^p$ using $\widehat{\mathbf{x}}_k^p$ and PCA transformation [16].
  if $\sum_{n=1}^{N} Erem_k(n) > 0$ **then** `(Prediction step)`
    Initialize $M_{k+1|k}^p \leftarrow M_k^p$.
    Compute $\widehat{\delta}_k^p$ (Sec. III).
    if $\widehat{\delta}_k^p > \delta_{th}^p$ **then**
      $M_{k+1|k}^p \leftarrow M_k^p + 1$.
    else
      for $i = 1, \ldots, M_k^p - R$ **do**
        Construct $\mathcal{A}_{k|M_k^p-i}^p$ (Sec. III), $\mathbf{A}_{k|M_k^p-i}^p$.
        Obtain $\widehat{\mathbf{x}}_{k|M_k^p-i}^p$using SBL.
        Compute $\text{BCRB}_{k|M_k^p-i}^p$, $\widehat{\epsilon}_k^p$ (Sec. III).
        if $\widehat{\epsilon}_k^p \leq \epsilon_{th}^p$ and $\text{BCRB}_{k|M_k^p-i}^p \in [\alpha, \beta]$ **then**
          $M_{k+1|k}^p \leftarrow M_k^p - i$.
        else if $\text{BCRB}_{k|M_k^p-i}^p \notin [\alpha, \beta]$ **then** $break$.
        end if
      end for
    end if
    Update:$\mathbf{B}_{k+1}^p$(use $\widehat{\mathbf{z}}_k^p$ in PCA). `(Update step)`
    Obtain $\mathcal{I}_{k+1|k}^p$ using (9).
    do
      Call Alg. Modified Binary Search [16] with inputs $\mathbf{Erem}_k, \mathbf{B}_{k+1}^p, M_{k+1|k}^p, \mathcal{I}_{k+1|k}^p, \forall p$.
      if $\sum_{n=1}^{N} \widetilde{\mathbf{A}}_{k+1}^p(n,n) == M_{k+1|k}^p$ **then**
        Obtain $\mathcal{A}_{k+1}^p, \mathbf{A}_{k+1}^p$.
        Calc. BCRB_{k+1}^p (Sec. III).
        if $\text{BCRB}_{k+1}^p < \alpha$ **then**
          $M_{k+1|k}^p \leftarrow \max\left\{M_{k+1|k}^p - 1, R\right\}$.
        else if $\text{BCRB}_{k+1}^p > \beta$ **then**
          $M_{k+1|k}^p \leftarrow \min\left\{M_{k+1|k}^p + 1, N\right\}$.
        end if
      else
        $exitflag^p \leftarrow 1$, $break$.
      end if
    while $\text{BCRB}_{k+1}^p \notin [\alpha, \beta]$.
    Update: $M_{k+1}^p \leftarrow M_{k+1|k}^p$.
  else
    $exitflag^p \leftarrow 1$.
  end if
  Update: $k \leftarrow k+1$.
end while
Output: $K = k$.

IV. Simulation Results and Discussion

This section demonstrates via simulations the sensing quality and energy efficiency of the proposed multi-sensing framework over the existing monolithic sensing scheme proposed by Chen *et al.* [12], [13]. Note that, the novel multi-sensing framework with EH-capable wireless nodes proposed herein, is not the agenda in [12], [13]. The approach in [12], [13] is considered as the closest benchmark because it proposed subset selection for optimal sensing. For a fair comparison, EH-capability, SBL-based recovery, and BCRB measure are incorporated in Chen's approach [12], [13] as well.

[1]This heuristic determines amount by which M_k^p can be decreased for next $(k+1)^{th}$ cycle such that the estimates $\widehat{\mathbf{x}}_k^p$ and $\widehat{\mathbf{x}}_{k|M_k^p-i}^p$ are nearly same.

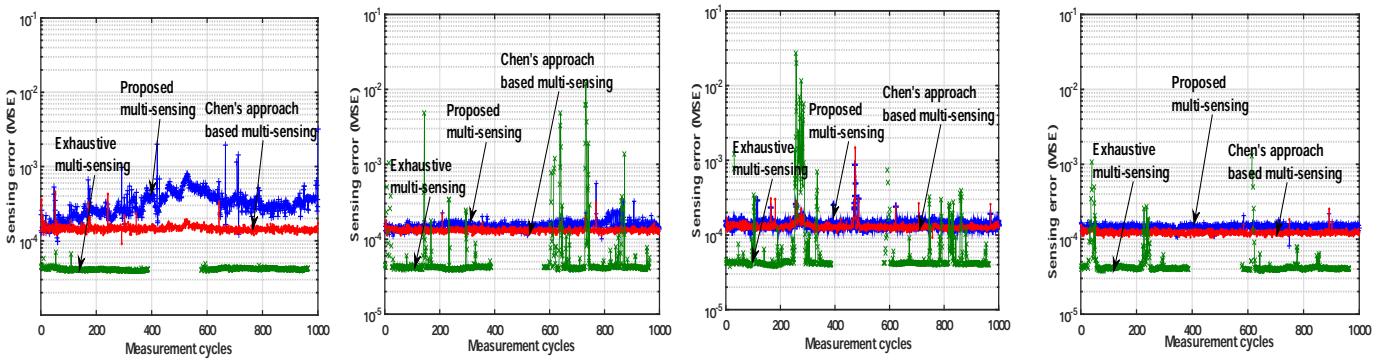

(a) CO (b) SO_2 (c) NO_2 (d) H_2S

Fig. 3: Comparison of sensing error resulted while sensing (a) CO, (b) SO_2, (c) NO_2, and (d) H_2S gases using the proposed adaptive multi-sensing framework and Chen's framework [12], [13] ($\{M_k^p, \forall p\} = \{17, 19, 20, 21\}, \forall k$ measurement cycles).

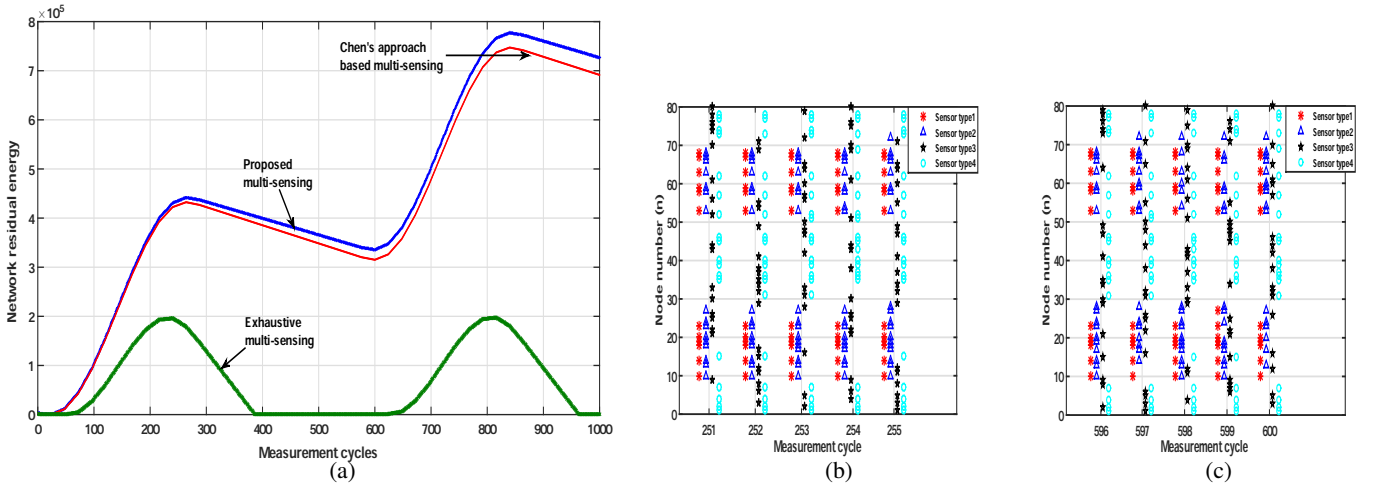

(a) (b) (c)

Fig. 4: (a) Comparison of network residual energy using the proposed approach with Chen's framework [12], [13] and exhaustive multi-sensing. Sensor activation pattern in measurement cycles (b) $251-255$ and (c) $596-600$ using the proposed framework.

$N = 80$ solar EH nodes are considered deployed in a 2-dimensional WSN field of size 100×100 m^2 divided into $\lceil\sqrt{N}\rceil \times \lceil\sqrt{N}\rceil = 9 \times 9$ square areas of size $\approx 11 \times 11$ m^2 each, roughly containing one randomly deployed node [28]. The field is divided in $R = 4$ coverage regions. Initial energy of nodes is set as $Erem_1(\cdot) = 40$ J. Each node has $P = 4$ sensors for monitoring environment parameters, namely, CO, SO_2, NO_2, and H_2S pollutants, with respective sensing energies $\{E_s^p, 1 \le p \le P\} = \{0.2546, 4.8321, 10.8265, 2.6963\}$ J [23] and detection limits $\{\rho^p, 1 \le p \le P\} = \{0.04, 0.01, 0.02, 0.02\}$. In the simulation, $\rho^p, \forall p$, are fixed such that they lie within dynamic range of corresponding synthetically generated pollutant signals. However, these can be set as per specification provided in sensors data-sheets. $S^p = 1, \forall p$, sources of pollutants are assumed to be located at the center of the field and the FC is located at a distance 110 m above the center of the WSN field. Source signals are generated as $u_1^p \sim \mathcal{N}(0,1), \forall p$ [29]. Spatio-temporal parameters of pollutant sources are set as $\{\theta^p, 1 \le p \le P\} = \{100, 500, 1000, 5000\}$ and $\{\varphi^p, 1 \le p \le P\} = \{0.99, 0.92, 0.95, 0.98\}$. Noise variance is fixed as $\sigma^2 = 10^{-5}$. Parameter Δ in MBS [16] and $[\alpha, \beta]$ are respectively set as 10^{-6} and $\left[10^{-5}, 2.3 \times 10^{-4}\right]$. To capture pollution process dynamics effectively, the thresholds are set as $\{\delta_{th}^p, \forall p\} = \{0.11, 0.28, 0.23, 0.15\}$ and $\{\epsilon_{th}^p, \forall p\} = \left\{2.5 \times 10^{-5}, \forall p\right\}$. Further, performance measures used in simulation plots are, sensing error (MSE) $= \left\|\mathbf{x}_k^p - \widehat{\mathbf{x}}_k^p\right\|^2 = \left\|\mathbf{z}_k^p - \widehat{\mathbf{z}}_k^p\right\|^2$ and network residual energy in k^{th} cycle $= \sum_{n=1}^{N} Erem_k(n)$. (Since MSE cannot be computed at the receiver due to unavailability of $\mathbf{z}_k^p$, BCRB is adopted as the performance measure. The MSE plots are used just to show that the proposed framework still provides a stable sensing quality.) Signal estimation process is averaged over 300 Monte-Carlo iterations in each measurement cycle. The results discussed below are obtained by simulating the WSN field and proposed multi-sensing framework in Matlab.

For performance comparison, the parameters $[\alpha, \beta]$ in the proposed framework are set as per the minimum and maximum BCRB achieved in the competitive scheme [12], [13] and λ_1^p in (6) is set such that $\text{BCRB}_1^p \in [\alpha, \beta], \forall p$. Figs. 3(a)-(d) and 4(a) compare sensing quality and energy efficiency performances of the proposed multi-sensing framework with that of the closest monolithic sensing approach [12], [13] by running it separately for P pollutants. Exhaustive sensing approach (sense using all nodes' sensors) is also compared herein. The proposed framework provides stable sensing quality (Fig. 3(a)-(d)) and is 4.58% and 98.92% energy-efficient compared to the approach [12], [13] and exhaustive sensing respectively (Fig. 4(a)). Gain in energy efficiency is due to optimized selection of sensors of each type without significantly trading

off their sensing quality. Low MSE achieved for all pollutant cases ($< 10^{-3}$) is due to sensor selection based on chosen $[\alpha, \beta]$ and usage of an efficient recovery algorithm (SBL). Increasing trend in the network residual energy is due to harvested solar energy pattern plotted in Fig. 2. Note that, discontinuities in the MSE plots corresponding to exhaustive multi-sensing are due to no sensing and signal estimation operations conducted in some measurement cycles owing to zero network residual energy. In the proposed framework, such discontinuities are seen when a pollutant signal is below detection limit of corresponding sensor of all nodes, due to which estimation process is not carried out in that cycle. Next, Fig. 4(b)-(c) shows active sensors of all the nodes obtained in the measurement cycles $251 - 255$ and $596 - 600$ using the proposed framework. Here, red/blue/black/cyan color marks across any n^{th} node represents active type 1 (CO)/type 2 (SO_2)/type 3 (NO_2)/type 4 (H_2S) sensor of that node in the corresponding cycle. Sensor activation varies from cycle to cycle as it depends on WSN topology and pollutant sources' locations (considered fixed), corresponding node's remaining and harvested energy, and spatio-temporal profile of pollutants.

Remark: *Proposed framework offers energy-efficient multi-sensing within a sensing accuracy limit in a heterogeneous EH-WSN; it is of interest in smart environment monitoring.*

V. Conclusion

This paper has proposed a novel adaptive multi-sensing framework for energy harvesting heterogeneous WSN used in smart environment applications of IoT. The framework dynamically adapts and computes optimized active sensors sets of the field nodes for monitoring different environment parameters simultaneously. For active set selection of each type of sensor, a critical trade-off between sensing quality and energy efficiency has been jointly optimized. The framework has incorporated system constraint imposed by different detection limits of the sensors along with stochastic solar energy availability. Simulation studies of the proposed framework has demonstrated its consistently-superior system performance with respect to the conventional exhaustive sensing as well as the closest available subset selection framework.

Acknowledgment

This work has been supported in parts by the Department of Science and Technology, International Bilateral Cooperation Division, under the Grant no. INT/UK/P-153/2017, the Department of Telecommunications, under the Grant no. 4-23/5G test bed/2017-NT for building end to end 5G test-bed, and TCS RSP Fellowship.

References

[1] A. De Paola, P. Ferraro, S. Gaglio, G. L. Re, and S. K. Das, "An adaptive Bayesian system for context-aware data fusion in smart environments," *IEEE Trans. Mobile Comput.*, vol. 16, no. 6, pp. 1502–1515, 2017.

[2] S. De and R. Singhal, "Toward uninterrupted operation of wireless sensor networks," *IEEE Computer Mag.*, vol. 45, no. 9, pp. 24–30, 2012.

[3] S. Suman, S. Kumar, and S. De, "Path loss model for UAV-assisted RFET," *IEEE Commun. Lett.*, vol. 22, no. 10, pp. 2048–2051, 2018.

[4] S. Sudevalayam and P. Kulkarni, "Energy harvesting sensor nodes: Survey and implications," *IEEE Commun. Surveys and Tuts.*, vol. 13, no. 3, pp. 443–461, 2011.

[5] M. V. Ramesh and V. P. Rangan, "Data reduction and energy sustenance in multisensor networks for landslide monitoring," *IEEE Sensors J.*, vol. 14, no. 5, pp. 1555–1563, 2014.

[6] Q. Ling and Z. Tian, "Decentralized sparse signal recovery for compressive sleeping wireless sensor networks," *IEEE Trans. Signal Process.*, vol. 58, no. 7, pp. 3816–3827, 2010.

[7] T. Xue, X. Dong, and Y. Shi, "Multiple access and data reconstruction in wireless sensor networks based on compressed sensing," *IEEE Trans. Wireless Commun.*, vol. 12, no. 7, pp. 3399–3411, 2013.

[8] Y. Chen and Q. Zhao, "On the lifetime of wireless sensor networks," *IEEE Commun. Lett.*, vol. 9, no. 11, pp. 976–978, 2005.

[9] S. Joshi and S. Boyd, "Sensor selection via convex optimization," *IEEE Trans. Signal Process.*, vol. 57, no. 2, pp. 451–462, 2009.

[10] S. Hwang, R. Ran, J. Yang, and D. K. Kim, "Multivariated Bayesian compressive sensing in wireless sensor networks," *IEEE Sensors J.*, vol. 16, no. 7, pp. 2196–2206, 2015.

[11] S. P. Chepuri and G. Leus, "Sparsity-promoting sensor selection for non-linear measurement models," *IEEE Trans. Signal Process.*, vol. 63, no. 3, pp. 684–698, 2015.

[12] W. Chen and I. J. Wassell, "Compressive sleeping wireless sensor networks with active node selection," in *Proc. IEEE Global Commun. Conf. (GLOBECOM)*. Austin, TX, USA, 2014, pp. 7–12.

[13] ——, "Optimized node selection for compressive sleeping wireless sensor networks," *IEEE Trans. Veh. Technol.*, vol. 65, no. 2, pp. 827–836, 2016.

[14] G. Quer, R. Masiero, G. Pillonetto, M. Rossi, and M. Zorzi, "Sensing, compression, and recovery for WSNs: Sparse signal modeling and monitoring framework," *IEEE Trans. Wireless Commun.*, vol. 11, no. 10, pp. 3447–3461, 2012.

[15] J. Hao, B. Zhang, Z. Jiao, and S. Mao, "Adaptive compressive sensing based sample scheduling mechanism for wireless sensor networks," *Pervasive and Mobile Comput.*, vol. 22, pp. 113–125, 2015.

[16] V. Gupta and S. De, "SBL-based adaptive sensing framework for wsn-assisted iot applications," *IEEE Internet of Things J.*, 2018.

[17] D. Bri, H. Coll, M. Garcia, and J. Lloret, "A multisensor proposal for wireless sensor networks," in *IEEE Int. Conf. Sensor Tech. and Appl. (SENSORCOMM)*. Cap Esterel, France, 2008, pp. 270–275.

[18] M. A. Akbar, A. A. S. Ali, A. Amira, M. Benammar, F. Bensaali, S. Mohamad, F. Tang, A. Bermak, M. Zgaren, and M. Sawan, "A multi-sensing reconfigurable platform for gas applications," in *IEEE Int. Conf. Microelec. (ICM)*. Doha, Qatar, 2014, pp. 148–151.

[19] Z. Zhu and S. O. Oyadiji, "Structure design of wireless sensor nodes with energy and cost awareness for multichannel signal measurement," *ACM Trans. Embedded Comput. Sys. (TECS)*, vol. 15, no. 1, p. 16, 2016.

[20] R. Prabha, M. V. Ramesh, V. P. Rangan, P. Ushakumari, and T. Hemalatha, "Energy efficient data acquisition techniques using context aware sensing for landslide monitoring systems," *IEEE Sensors J*, vol. 17, pp. 6006–6018, 2017.

[21] C. R. Rao, "The use and interpretation of principal component analysis in applied research," *Sankhyā: The Indian Jour. Statistics, Ser. A*, pp. 329–358, 1964.

[22] A. Caruso, S. Chessa, S. Escolar, X. del Toro, and J. C. López, "A dynamic programming algorithm for high-level task scheduling in energy harvesting IoT," *IEEE Internet of Things J.*, 2018.

[23] P. Gupta, K. Kandakatla, S. De, and S. Jana, "Feasibility analysis on integrated recharging and data collection in pollution sensor networks," in *Nat. Conf. Commun. (NCC)*. New Delhi, India, 2013, pp. 1–5.

[24] S. S. Chandel and R. K. Aggarwal, "Estimation of hourly solar radiation on horizontal and inclined surfaces in western himalayas," *Smart grid and renewable energy*, vol. 2, no. 01, p. 45, 2011.

[25] D. P. Wipf and B. D. Rao, "Sparse Bayesian learning for basis selection," *IEEE Trans. Signal Process.*, vol. 52, no. 8, pp. 2153–2164, Aug. 2004.

[26] Z. Fei, B. Li, S. Yang, C. Xing, H. Chen, and L. Hanzo, "A survey of multi-objective optimization in wireless sensor networks: metrics, algorithms, and Open Problems," *IEEE Commun. Surveys and Tuts.*, vol. 19, no. 1, pp. 550–586, 2017.

[27] I. CVX Research, "CVX: Matlab software for disciplined convex programming, version 2.0," http://cvxr.com/cvx, Aug. 2012.

[28] M. Leinonen, M. Codreanu, and M. Juntti, "Sequential compressed sensing with progressive signal reconstruction in wireless sensor networks," *IEEE Trans. Wireless Commun.*, vol. 14, no. 3, pp. 1622–1635, 2015.

[29] J. V. Zidek, W. Sun, and N. D. Le, "Designing and integrating composite networks for monitoring multivariate Gaussian pollution fields," *Jour. Royal Statistical Soc.: Ser. C*, vol. 49, no. 1, pp. 63–79, 2000.